

<https://helda.helsinki.fi>

Computed Pre-reactive Complex Association Lifetimes Explain Trends in Experimental Reaction Rates for Peroxy Radical Recombinations

Daub, Christopher David

2022-09-16

Daub , C D , Valiev , R , Salo , V-T , Zakai , I , Gerber , R B & Kurten , T 2022 , ' Computed Pre-reactive Complex Association Lifetimes Explain Trends in Experimental Reaction Rates for Peroxy Radical Recombinations ' , ACS Earth and Space Chemistry , vol. 6 , pp. 2446-2452 . <https://doi.org/10.1021/acsearthspacechem.2c00159>

<http://hdl.handle.net/10138/355838>

<https://doi.org/10.1021/acsearthspacechem.2c00159>

cc_by

publishedVersion

Downloaded from Helda, University of Helsinki institutional repository.

This is an electronic reprint of the original article.

This reprint may differ from the original in pagination and typographic detail.

Please cite the original version.

Computed Pre-reactive Complex Association Lifetimes Explain Trends in Experimental Reaction Rates for Peroxy Radical Recombinations

Christopher David Daub,* Rashid Valiev, Vili-Taneli Salo, Itai Zakai, R. Benny Gerber,* and Theo Kurtén*



Cite This: *ACS Earth Space Chem.* 2022, 6, 2446–2452



Read Online

ACCESS |

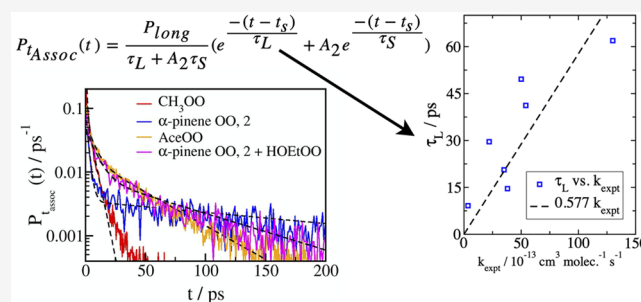
Metrics & More

Article Recommendations

Supporting Information

ABSTRACT: The lifetimes of pre-reactive complexes, although implicitly part of the equations used to model many gas-phase bimolecular reactions, have seldom been included in quantitative calculations of rate coefficients. Here, we demonstrate the application of empirical molecular dynamics simulations of collisions between peroxy radicals to model association lifetimes. With the exception of the methyl peroxy–acetyl peroxy system, measurements of the lifetimes based on a phenomenological model are shown to correlate well with available experimental data for recombination reactions of peroxy radicals in cases where the rate-limiting transition state lies below the reactants in energy. Further, we predict reaction rates for larger α -pinene-derived peroxy radicals, and we interpret our results in tandem with available experimental data on these systems, which are of great relevance to improve our understanding of atmospheric aerosol formation.

KEYWORDS: peroxy radicals, aerosol, reaction kinetics, Arrhenius equation, α -pinene



1. INTRODUCTION

Peroxy radicals with general formula RO_2 are important intermediates formed by oxidation of many organic compounds when exposed to molecular oxygen. In the gas phase, RO_2 radicals are long-lived compared to other radicals, with a complicated chemistry usually dominated by bimolecular reactions, either with other small molecules or radicals, such as NO or HO_2 , or during self- and cross-reactions with the same or other peroxy radicals.¹ These reactions with other peroxy species are of particular interest as a result of the possibility of forming stable low-volatility accretion products, such as ROOR species, which play a role in atmospheric new-particle formation and aerosol growth.^{2–4} The atmospheric chemistry of larger peroxy radicals formed from oxidation of α -pinene and other terpenes^{5,6} or from isoprene^{7,8} has received a great deal of recent attention.

In recent work, we and others have used computational methods to study the energetics^{9–13} of peroxy radical self- and cross-reactions. Very recently, we also extended our work to include dynamics.¹⁴ In this study, we used molecular dynamics (MD) simulations in combination with three different approaches to energy and gradient calculations. High-level calculations using the second-order perturbation theory (XMC-QDPT2)¹⁵ confirmed the results of a previous work,¹¹ showing that, for the simplest methyl peroxy radical, the formation of a tetroxide intermediate ($\text{CH}_3\text{O}_4\text{CH}_3$) takes

place rapidly and with effectively no energetic barrier (because the rate-limiting transition state is submerged, i.e., lies well below the free reactants in energy). Semi-empirical calculations based on the orthogonalization-corrected modified neglect of diatomic overlap (MNDO) theory¹⁶ generally agreed with the high-level fully *ab initio* results and allowed us to explore a more varied conformational space with considerably cheaper methods, including a realistic treatment of molecular collisions. Finally, we were able to use simple empirical force fields based on the optimized potentials for liquid simulations (OPLS) framework to describe non-reactive collisions between peroxy radicals, including larger systems, which we were not able to deal with using more expensive methods. It is the empirical simulations that we focus on here.

In the previous work,¹⁴ we noted that the results of force-field-based MD simulations for methyl peroxy collisions agreed very well with the results of semi-empirical-based MD simulations on the triplet potential energy surface. This surface is non-reactive; therefore, it allows for direct comparison to

Received: May 26, 2022

Revised: August 5, 2022

Accepted: September 6, 2022

Published: September 16, 2022



non-reactive force-field-based methods. With extension to other peroxy systems, we also studied acetonyl peroxy and *t*-butyl peroxy collisions. For *t*-butyl peroxy, we found that the distribution of association times was rather similar to methyl peroxy. On the other hand, acetonyl peroxy collisions had a significantly higher chance to remain associated for a longer time. We noted that this was consistent with the fact that the self-reaction rate of acetonyl peroxy radicals has been experimentally found to be $\sim 10\text{--}20\times$ higher than that of methyl peroxy radicals.^{1,17,18} On the basis of both computations¹³ and experimentally determined effective activation energies,¹ acetonyl peroxy, like methyl peroxy, is found to have a negligible energy barrier, while *t*-butyl peroxy has a barrier of several kcal/mol.

The behavior of pre-reactive complexes is implicitly included in the theoretical descriptions of chemical reactions, e.g., in the pre-exponential factor *A* in the Arrhenius equation.

$$k = Ae^{-E_a/k_B T} \quad (1)$$

However, attempts to model and/or predict the pre-exponential factor in a quantitative fashion are few and far between, especially where complex polyatomic molecules are involved. The main goal of the current study is to develop a more general and quantitative model to describe the association time histograms of pre-reactive complexes and then to further examine whether a computation of such histograms can be used to predict experimental rate coefficients for a wider variety of peroxy radicals, at least in cases where no significant energetic reaction barrier exists (i.e., where a rate-limiting transition state either does not exist at all or is submerged). On the basis of the empirical activation energies reported in Table 7 by Orlando et al.,¹ this should apply to at least self-reactions of methyl peroxy (CH₃OO or MeOO), ethanol peroxy [HO(CH₂)₂OO or HOEtOO], chloromethyl peroxy (ClCH₂OO), acetyl peroxy [CH₃C(O)OO or AcOO], and acetonyl peroxy [CH₃C(O)CH₂OO or AceOO] as well as the cross-reactions between MeOO, AcOO, and AceOO, among others.

2. METHODS AND MODELS

The empirical force fields that we use to describe the systems of peroxy radicals are based on the OPLS models.^{19–21} The force field for the simplest methyl peroxy system was assembled manually on the basis of the published all-atom optimized potentials for liquid simulations (OPLS-AA) parameters.²⁰ For all others, we used the LigParGen web server to automatically generate large-scale atomic/molecular massively parallel simulator (LAMMPS) data files for ROOH molecules,^{22,23} with partial charges computed at the CM1A level and scaled by a factor of 1.14. Because parameters for peroxy oxygens are not available in the standard OPLS framework, we manually removed peroxide hydrogen, modified the force field with non-bonded, bonded, and angular terms developed in another work on peroxy radicals,²⁴ and finally altered the charge of the carbon atom closest to the peroxy group to maintain overall charge neutrality.

MD simulations were run with a recent version of LAMMPS.²⁵ We generate collisions between radicals in the same way as in our previous work.¹⁴ Briefly, two molecules are placed some distance apart (varying from 35 Å for smaller species up to 60 Å for α -pinene peroxy collisions) and given random orientations. After a short equilibration to ensure the initial temperature of each molecule of $T \sim 300$ K, one

molecule is given a center of mass velocity in the direction of the center of mass of the other molecule. The collision velocity is $v_z = 520$ m/s for methyl peroxy, near the expected relative velocity of two methyl peroxy radicals calculated from a Boltzmann distribution at 300 K. The velocity of other species is scaled, so that the translational kinetic energy is the same for methyl peroxy.

The simulation time step is $dt = 0.2$ fs in all cases (a test run of 10 000 collisions of the methyl peroxy system with $dt = 0.1$ fs showed no significant differences). The total simulation time for each collision ranged from 200 ps for methyl and other relatively simple peroxy radicals up to 800 ps for some of the α -pinene-derived peroxy radicals. These trajectories are long enough to observe the initial collision and association and, except in rare cases, the eventual dissociation and separation of the two radicals. Our data for methyl, acetonyl, and *t*-butyl peroxy collisions come from our previous work,¹⁴ while data for other species are new. In all, 30 000 trajectories were analyzed for methyl peroxy, with 20 000 for each of the other small peroxy species, 3500 for each of the larger α -pinene-derived species, and 5000 for collisions between α -pinene peroxys and HOEtOO. LAMMPS “input” and “data” files, which can be used to start a single collision trajectory for each system, are provided in the [Supporting Information](#).

Trajectory analysis of collisions between the radicals is used to compute the association time t_{Assoc} of the pre-reactive complex during each collision. This is defined as the difference between the first and last times that $r_{\text{min}} < 4.0$ Å, where r_{min} is the smallest interatomic distance between heavy (non-hydrogen) atoms in different molecules. This is a less restrictive definition of a pre-reactive complex than that commonly used in quantum chemistry, where defined pre-reactive complex geometries are found by optimization.

In our previous work,¹⁴ we have recognized that a probability density histogram of t_{Assoc} computed over a sufficient number of collisions generally features an initial peak in the probability distribution, corresponding to roughly elastic collisions, which last less than ~ 2 ps. Subsequently, there is a smooth monotonic decrease in the probability of longer t_{Assoc} . Including the initial peak in the probability histogram in a simple phenomenological model would be a challenge, and we do not attempt to do so. Instead, in our model, we only attempt to fit the probability distribution of t_{Assoc} for $t > t_s$, where we have set $t_s = 2$ ps. We base this on the likelihood that very short-lived collisions with duration of $< t_s$ do not form any kind of pre-reactive complex and, hence, are unreactive. This value of t_s works well for all of the cases that we study here; it is possible that collisions between larger molecules, for example, might require t_s to have a larger value.

For $t > t_s$, we fit a simple biexponential model with four parameters.

$$P_{t_{\text{Assoc}}}(t) = A_1(e^{-(t-t_s)/\tau_L} + A_2e^{-(t-t_s)/\tau_S}) \quad (2)$$

Furthermore, because $\int_{t_s}^{\infty} P_{t_{\text{Assoc}}}(t) dt = P_{\text{long}}$, where P_{long} is the total probability that a collision lasts longer than t_s , we can eliminate one fitting parameter, leading to a new equation.

$$P_{t_{\text{Assoc}}}(t) = \frac{P_{\text{long}}}{\tau_L + A_2\tau_S}(e^{-(t-t_s)/\tau_L} + A_2e^{-(t-t_s)/\tau_S}) \quad (3)$$

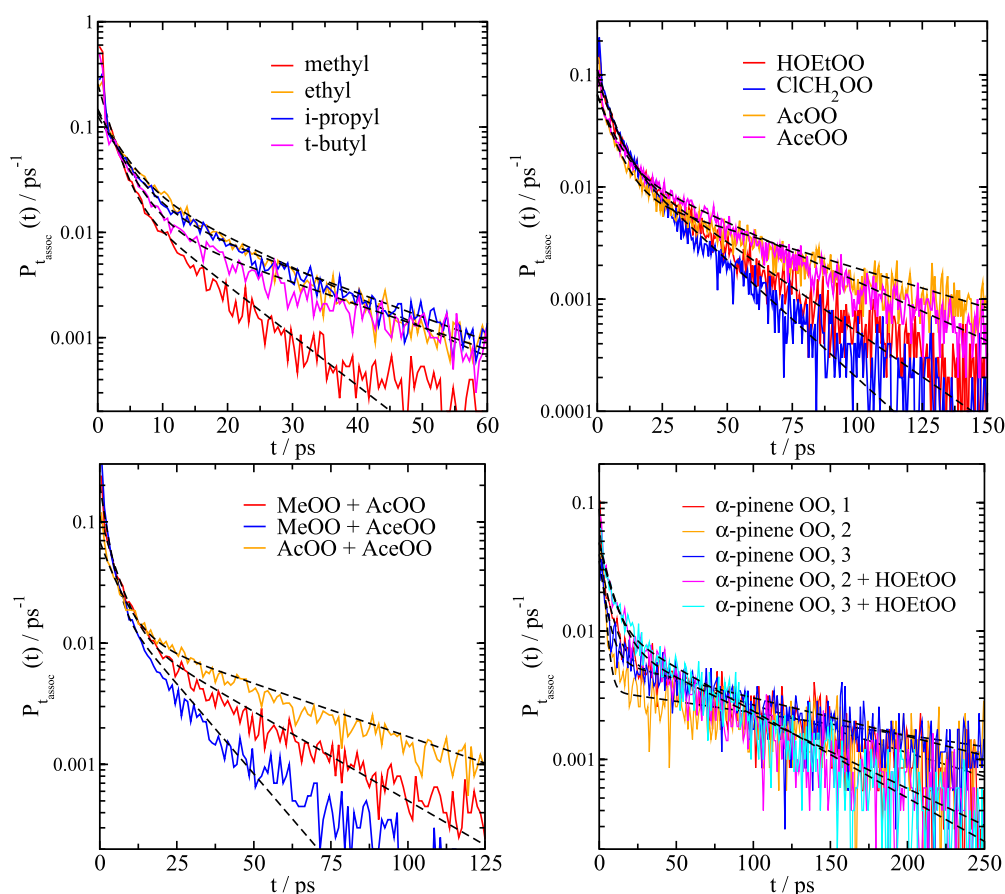


Figure 1. Plots of the fits of our model (eq 3) to the distributions of association times: (upper left) hydrocarbon-based peroxy radicals (RO_2 , where $R = \text{Me, Et, i-Pr, and } t\text{-Bu}$), (upper right) $\text{HO}(\text{CH}_2)_2\text{OO}$, ClCH_2OO , AcOO , and AceOO , (lower left) cross-reactions between MeOO , AcOO , and AceOO , and (lower right) α -pinene-based peroxy radical self- and cross-reactions with $\text{HO}(\text{CH}_2)_2\text{OO}$.

Table 1. Fitting Parameters Used in Eq 3 and Available Experimental Rate Constants k_{expt}^a

system	$k_{\text{expt}} (\times 10^{-13}, \text{cm}^3 \text{ molecule}^{-1} \text{ s}^{-1})$	P_{long}	τ_L (ps)	A_2	τ_S (ps)
MeOO	3.5	0.342	9.2	3.4	1.8
EtOO*	0.76	0.628	15.4	2.0	3.2
i-PrOO*	0.01	0.585	18.9	3.0	3.6
<i>t</i> -BuOO*	2.1×10^{-5}	0.489	20.4	5.3	3.1
HOEtOO	22	0.761	27.2	2.7	5.0
ClCH_2OO	35	0.717	20.6	2.4	4.5
AcOO	160 and 130^{26}	0.795	61.9	4.4	5.7
AceOO	80, 48, ¹⁷ and 54^{18}	0.834	41.2	2.2	5.7
MeOO + AcOO	110 and 200^{26}	0.667	29.6	4.4	4.3
MeOO + AceOO	38^{18}	0.502	14.6	3.4	2.4
AcOO + AceOO	50^{18}	0.812	49.6	3.2	5.3
α -pinene OO, 1	NA	0.853	117	3.8	5.7
α -pinene OO, 2	NA	0.919	247	9.7	2.1
α -pinene OO, 3	NA	0.939	145	3.1	4.3
α -pinene OO, 2 + HOEtOO	NA	0.849	76	3.8	7.5
α -pinene OO, 3 + HOEtOO	NA	0.876	64	2.5	6.4

^aExperimental data are taken from ref 1, unless otherwise noted. Systems marked with an asterisk are known to have significant energetic barriers for recombination reactions.

3. RESULTS

As a result of the non-linearity of the model presented in eq 3, there is not a unique set of fit parameters that is guaranteed to be best. However, with judicious initial guesses for the parameters, we consistently see that the two exponential decay parameters τ_L and τ_S correspond to longer and shorter

decay time scales, respectively, while A_2 determines the relative contribution of the two decay processes. We see that this model fits the data reasonably well for t_{Assoc} ranging from 2 ps up to times corresponding to very low probability (this varies greatly with the system, from ~ 50 ps for simpler peroxy radicals up to ~ 300 ps or more for α -pinene-derived peroxy

radicals). We show graphs of all of our fits in Figure 1 and a table of fitting parameters and values of P_{long} in Table 1.

Reactions must result from sufficiently long-lasting complex associations, which have enough time to rearrange into the $\text{RO}_2\text{R}'$ geometry. Therefore, it is reasonable to interpret τ_L as a lifetime for a long-lived complex and, hence, as the most important factor for determining the reactivity, given that a collision has happened in the first place and that the reaction does not have a significant energetic barrier. In Figure 2, we

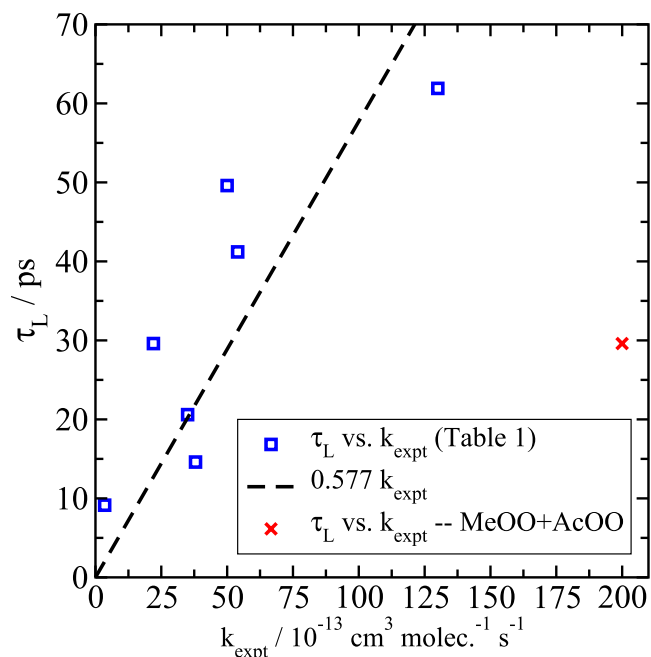


Figure 2. Correlation between τ_L measured in collision simulations versus values of k_{expt} . The data point for MeOO + AcOO is shown by the red \times symbol and is not included in the fit. Experimental data used in the fit are the most recent available numbers from Table 1.

plot the values of τ_L measured in our simulations versus k_{expt} taken from ref 1 only for those reactions that do not feature any energetic barrier according to the experimental data (for the ethyl, *i*-propyl, and *t*-butyl cases, experimental activation energies indicate the existence of a substantial barrier, explaining the lack of correlation between the rate coefficient and the complex lifetime).

For the most part, we see that there is a reasonable trend, whereby longer association lifetimes τ_L computed with our model correlate with higher experimental reactivity k_{expt} . However, there is clearly an outlier in the case of MeOO + AcOO. Recent experiments²⁶ have measured a surprisingly

high reactivity for this cross-reaction ($k = 200 \times 10^{-13} \text{ cm}^{-3} \text{ molecule}^{-1} \text{ s}^{-1}$), even higher than the reactivity of the AcOO self-reaction ($k = 130 \times 10^{-13} \text{ cm}^{-3} \text{ molecule}^{-1} \text{ s}^{-1}$). Our modeling would instead be consistent with a value of k for the cross-reaction in between the values for MeOO and AcOO self-reactions. This intuitive prediction is also consistent with our recent calculations of the energetics in these systems.¹³ We also note that a semi-empirical calculation of k for the MeOO + AcOO cross-reaction arrived at a value of $70 \times 10^{-13} \text{ cm}^{-3} \text{ molecule}^{-1} \text{ s}^{-1}$,²⁷ which would fall in line with our model. Clearly, there is more work to be done to successfully understand this particular system.

Excluding only the MeOO + AcOO system, we observe a significant degree of correlation ($r = 0.845$) between τ_L and k_{expt} . A simple linear fit suggests a relation of $\tau_L = 0.577k_{\text{expt}}$ with units given in Figure 2. Given the inherent limitations of the OPLS-based empirical force fields that we used, the simplicity of the fitting model, and the fact that the k_{expt} values themselves may only be accurate within 50% or worse,¹ this is a remarkable and useful result.

Assuming this correlation can also be applied to other peroxy radicals, given a measurement of the complex lifetime τ_L , we can predict experimental rate constants for systems where these data are partially or completely lacking. Here, we present our predictions for self-reactions of atmospherically relevant α -pinene-derived peroxy radicals as well as their cross-reactions with HOEtOO. We investigate three different radicals, with optimized structures shown in Figure 3. These structures were generated by running MD simulations using LAMMPS at $T = 5 \text{ K}$, starting from structures optimized using quantum chemical methods previously.²⁸ Radical 1 is the main first-generation peroxy radical produced in OH-initiated oxidation of α -pinene, while radicals 2 and 3 are two of the four^{29–31} (or possibly five²⁸) main first-generation peroxy radicals produced in α -pinene ozonolysis. We caution that, because radical 1 is a tertiary peroxy radical, its reactions may be associated with a substantial barrier. The rates predicted here should thus be considered upper limits, especially for radical 1.

The lifetime of α -pinene-based peroxy radical complexes is predicted to be significantly longer than for the smaller species. Accordingly, their reactivity should be higher. Predictions of the total reaction rate for these $k_{\text{pred}} = (\tau_L/0.577) \times 10^{-13} \text{ cm}^{-3} \text{ molecule}^{-1} \text{ s}^{-1}$ (with τ_L measured in picoseconds) are given in Table 2. The increase in pre-reactive complex lifetimes with increasing functionalization may help explain both the trend in overall RO_2 self-reaction rates for primary and secondary systems reported by Orlando and Tyndall¹ and the remarkable

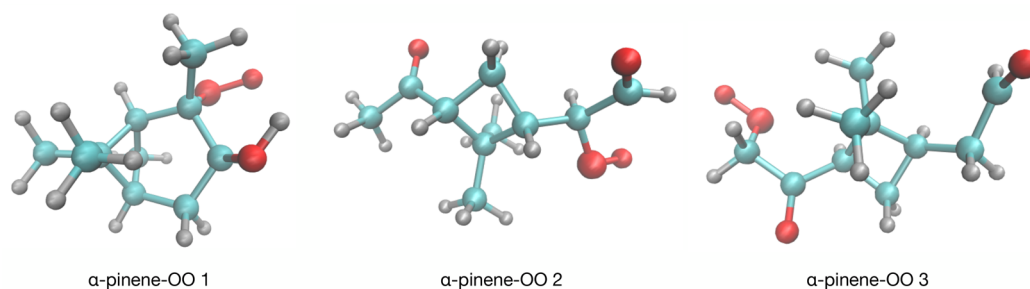


Figure 3. Three variants of α -pinene peroxy radicals that we studied. Structures are snapshots from LAMMPS simulations at $T = 5 \text{ K}$.

Table 2. Predicted Experimental Rate Constants k_{pred} for α -Pinene-Derived Peroxy Radical Recombination (with the Assumption of Submerged Barriers) and Available Experimental Data for ROOR' Formation k_{ROOR} from Berndt et al.^{4,a}

system	τ_L (ps)	$k_{\text{pred}} = (\tau_L/0.577) (\times 10^{-13}, \text{cm}^3 \text{molecule}^{-1} \text{s}^{-1})$	$k_{\text{ROOR}} (\times 10^{-13}, \text{cm}^3 \text{molecule}^{-1} \text{s}^{-1})$
α -pinene OO, 1	117	203	NA
α -pinene OO, 2	247	428	97
α -pinene OO, 3	145	251	97
α -pinene OO, 2 + HOEtOO	76	132	170
α -pinene OO, 3 + HOEtOO	64	111	170

^aNote that the experimental data do not distinguish between different structural isomers of α -pinene peroxy with the same mass.

increase in the effective rates of ROOR accretion product formation with chemical complexity reported by Berndt et al.³

Experimental data for all of the relevant reaction channels in the α -pinene-derived systems or even for the overall reaction rates are not available. However, there are some data on effective rate coefficients for the formation of ROOR' products.⁴ This is generally thought¹ to be one of the three main reaction channels for $\text{RO}_2 + \text{RO}_2'$ reactions, with the two other well-known channels corresponding to the formation of either alkoxy radicals or alcohol + carbonyl products. Table 2 includes these data for comparison purposes. Because only one of the reaction channels is included, our values of k_{pred} are expected to be above the experimental value of k_{ROOR} . However, on the basis of the observation of efficient ROOR' formation for complex systems,³ we also expect the two rates to be of the same order of magnitude. The results in Table 2 match both these expectations for the self-reactions, providing additional validation for the approach proposed here. However, the values of k_{pred} that we compute for the HOEtOO + α -pinene OO cross-reactions are somewhat lower than the experimental values of k_{ROOR} .

If we further assume that our values of k_{pred} are at least somewhat accurate, we can even use them to derive predictions for the branching ratios R between the ROOR' reactions and the total of all available reaction channels, $R = k_{\text{ROOR}}/k_{\text{pred}}$. This yields R values between 0.25 and 0.4 for the α -pinene OO self-reactions. For the α -pinene OO + HOEtOO cross-reactions, on the other hand, because values of k_{pred} are somewhat below k_{ROOR} , this would suggest that $R \approx 1$. While we caution that this difference may simply be a result of inaccuracies in our k_{pred} values, the result may also indicate that other reaction channels are less active for the α -pinene OO + HOEtOO reaction, for example, as a result of hydrogen bonds involving the OH group preventing the escape of alkoxy radicals.

4. CONCLUSION

In this work, we have undertaken a new approach to predict reaction rates for systems where energetic barriers are either non-existent or submerged. We used simple and inexpensive empirical force-field-based models to simulate thousands of collisions between peroxy radicals. Our phenomenological model (eq 3) of the probability histogram for the association time was used to determine a time scale τ_L describing the lifetime of pre-reactive complexes. In most cases, a high degree of correlation was found between τ_L and experimental measurements of the reaction rates.

Despite the overall success of our model, some challenges remain. In particular, some of the cross-reactions between unlike peroxy radicals were not described well. This is clear from the fact that we had to exclude the MeOO + AcOO system from our fit in Figure 2. We also underpredicted the

reaction rate for cross-reactions between α -pinene OO and HOEtOO. One possibility is that OPLS-based force fields, being determined on the basis of single molecules, can be inaccurate for interactions between unlike molecules. We will consider improvements to our models in continuing work.

We look forward to the testing of our predictions by more experiments on the α -pinene-derived peroxy radicals. Our predictions of reaction rates for different atmospheric molecules can help with choosing likely experimental targets as well as informing better models for the role of these molecules in aerosol and cloud formation. To this end, we will examine more of the secondary and tertiary α -pinene-derived peroxy systems as well as the isoprene-derived peroxy radicals, for which some experimental data already exist.⁴

Another intriguing prospect for future developments would be to test the generality of our model relating measured pre-reactive lifetimes to the reactivity. In principle, there is no *a priori* reason why this simple model should not be applicable to any bimolecular gas-phase reaction where significant energetic barriers are not present. Any self-reactions between radical pairs could be worthwhile targets, because they tend to be barrierless.³² Examples include the atmospherically important Criegee intermediates, which have been studied in experiments.^{33–35}

■ ASSOCIATED CONTENT

SI Supporting Information

The Supporting Information is available free of charge at <https://pubs.acs.org/doi/10.1021/acsearthspacechem.2c00159>.

LAMMPS “input” and “data” files, which can be used to generate a single collision trajectory for each of the systems that we studied, with running multiple trajectories with randomized molecular orientations used to generate our histograms of complex association lifetimes (ZIP)

■ AUTHOR INFORMATION

Corresponding Authors

Christopher David Daub – Department of Chemistry, University of Helsinki, 00014 Helsinki, Finland; orcid.org/0000-0002-4290-9058; Email: christopher.daub@helsinki.fi

R. Benny Gerber – Fritz Haber Research Center and Institute of Chemistry, Hebrew University of Jerusalem, 91904 Jerusalem, Israel; Department of Chemistry, University of California, Irvine, Irvine, California 92697, United States; orcid.org/0000-0001-8468-0258; Email: bgerber@uci.edu

Theo Kurtén – Department of Chemistry, University of Helsinki, 00014 Helsinki, Finland; orcid.org/0000-0002-6416-4931; Email: theo.kurten@helsinki.fi

Authors

Rashid Valiev – Department of Chemistry, University of Helsinki, 00014 Helsinki, Finland; orcid.org/0000-0002-2088-2608

Vili-Taneli Salo – Department of Chemistry, University of Helsinki, 00014 Helsinki, Finland; orcid.org/0000-0003-1152-446X

Itai Zakai – Fritz Haber Research Center and Institute of Chemistry, Hebrew University of Jerusalem, 91904 Jerusalem, Israel; orcid.org/0000-0002-0543-6562

Complete contact information is available at:

<https://pubs.acs.org/10.1021/acsearthspacechem.2c00159>

Notes

The authors declare no competing financial interest.

ACKNOWLEDGMENTS

Christopher David Daub, Rashid Valiev, and Theo Kurtén thank the Jane and Aatos Erkko Foundation for financial support. Theo Kurtén and Rashid Valiev are also supported by the Academy of Finland (Centre of Excellence VILMA, Grant 346369). Itai Zakai and R. Benny Gerber are supported by the Israel Science Foundation Grant 593/20. Computing resources were supplied by Finland's Center for Scientific Computing (CSC).

REFERENCES

- (1) Orlando, J. J.; Tyndall, G. S. Laboratory studies of organic peroxy radical chemistry: An overview with emphasis on recent issues of atmospheric significance. *Chem. Soc. Rev.* **2012**, *41*, 6294–6317.
- (2) Bianchi, F.; Kurtén, T.; Riva, M.; Mohr, C.; Rissanen, M. P.; Roldin, P.; Berndt, T.; Crouse, J. D.; Wennberg, P. O.; Mentel, T. F.; Wildt, J.; Junninen, H.; Jokinen, T.; Kulmala, M.; Worsnop, D. R.; Thornton, J. A.; Donahue, N.; Kjaergaard, H. G.; Ehn, M. Highly Oxygenated Organic Molecules (HOM) from Gas-Phase Autoxidation Involving Peroxy Radicals: A Key Contributor to Atmospheric Aerosol. *Chem. Rev.* **2019**, *119*, 3472–3509.
- (3) Berndt, T.; Scholz, W.; Mentler, B.; Fischer, L.; Herrmann, H.; Kulmala, M.; Hansel, A. Accretion Product Formation from Self- and Cross-Reactions of RO₂ Radicals in the Atmosphere. *Angew. Chem., Int. Ed.* **2018**, *57*, 3820–3824.
- (4) Berndt, T.; Mentler, B.; Scholz, W.; Fischer, L.; Herrmann, H.; Kulmala, M.; Hansel, A. Accretion Product Formation from Ozonolysis and OH Radical Reaction of α -Pinene: Mechanistic Insight and the Influence of Isoprene and Ethylene. *Environ. Sci. Technol.* **2018**, *52*, 11069–11077.
- (5) Claffin, M. S.; Krechmer, J. E.; Hu, W.; Jimenez, J. L.; Ziemann, P. J. Functional Group Composition of Secondary Organic Aerosol Formed from Ozonolysis of α -Pinene Under High VOC and Autoxidation Conditions. *ACS Earth Space Chem.* **2018**, *2*, 1196–1210.
- (6) Molteni, U.; Simon, M.; Heinritzi, M.; Hoyle, C. R.; Bernhammer, A.-K.; Bianchi, F.; Breitenlechner, M.; Brilke, S.; Dias, A.; Duplissy, J.; Frege, C.; Gordon, H.; Heyn, C.; Jokinen, T.; Kurten, A.; Lehtipalo, K.; Makhmutov, V.; Petäjä, T.; Pieber, S. M.; Praplan, A. P.; Schobesberger, S.; Steiner, G.; Stozhkov, Y.; Tomé, A.; Tröstl, J.; Wagner, A. C.; Wagner, R.; Williamson, C.; Yan, C.; Baltensperger, U.; Curtius, J.; Donahue, N. M.; Hansel, A.; Kirkby, J.; Kulmala, M.; Worsnop, D. R.; Dommen, J. Formation of Highly Oxygenated Organic Molecules from α -Pinene Ozonolysis: Chemical Characteristics, Mechanism, and Kinetic Model Development. *ACS Earth Space Chem.* **2019**, *3*, 873–883.
- (7) Møller, K. H.; Bates, K. H.; Kjaergaard, H. G. The Importance of Peroxy Radical Hydrogen-Shift Reactions in Atmospheric Isoprene Oxidation. *J. Phys. Chem. A* **2019**, *123*, 920–932.
- (8) Link, M. F.; Nguyen, T. B.; Bates, K.; Müller, J.-F.; Farmer, D. K. Can Isoprene Oxidation Explain High Concentrations of Atmospheric Formic and Acetic Acid over Forests? *ACS Earth Space Chem.* **2020**, *4*, 730–740.
- (9) Ghigo, G.; Maranzana, A.; Tonachini, G. Combustion and atmospheric oxidation of hydrocarbons: Theoretical study of the methyl peroxy self-reaction. *J. Chem. Phys.* **2003**, *118*, 10575–10583.
- (10) Lee, R.; Gryn'ova, G.; Ingold, K. U.; Coote, M. L. Why are sec-alkylperoxy bimolecular self-reactions orders of magnitude faster than the analogous reactions of tert-alkylperoxyls? The unanticipated role of CH hydrogen bond donation. *Phys. Chem. Chem. Phys.* **2016**, *18*, 23673–23679.
- (11) Valiev, R. R.; Hasan, G.; Salo, V.-T.; Kubečka, J.; Kurtén, T. Intersystem Crossings Drive Atmospheric Gas-Phase Dimer Formation. *J. Phys. Chem. A* **2019**, *123*, 6596–6604.
- (12) Hasan, G.; Salo, V.-T.; Valiev, R. R.; Kubečka, J.; Kurtén, T. Comparing Reaction Routes for ³(RO ... OR') Intermediates Formed in Peroxy Radical Self- and Cross-Reactions. *J. Phys. Chem. A* **2020**, *124*, 8305–8320.
- (13) Salo, V.-T.; Valiev, R.; Lehtola, S.; Kurtén, T. Gas-Phase Peroxy Radical Recombination Reactions: A Computational Study of Formation and Decomposition of Tetroxides. *J. Phys. Chem. A* **2022**, *126*, 4046–4056.
- (14) Daub, C. D.; Zakai, I.; Valiev, R.; Salo, V.-T.; Gerber, R. B.; Kurtén, T. Energy transfer, pre-reactive complex formation and recombination reactions during the collision of peroxy radicals. *Phys. Chem. Chem. Phys.* **2022**, *24*, 10033–10043.
- (15) Granovsky, A. A. Extended multi-configuration quasi-degenerate perturbation theory: The new approach to multi-state multi-reference perturbation theory. *J. Chem. Phys.* **2011**, *134*, 214113.
- (16) Dral, P. O.; Wu, X.; Thiel, W. Semiempirical Quantum-Chemical Methods with Orthogonalization and Dispersion Corrections. *J. Chem. Theory Comput.* **2019**, *15*, 1743–1760.
- (17) Zuraski, K.; Hui, A. O.; Grieman, F. J.; Darby, E.; Møller, K. H.; Winiberg, F. A. F.; Percival, C. J.; Smarte, M. D.; Okumura, M.; Kjaergaard, H. G.; Sander, S. P. Acetyl Peroxy and Hydro Peroxy Self- and Cross-Reactions: Kinetics, Mechanism, and Chaperone Enhancement from the Perspective of the Hydroxyl Radical Product. *J. Phys. Chem. A* **2020**, *124*, 8128–8143.
- (18) Assali, M.; Fittschen, C. Self-Reaction of Acetyl Peroxy Radicals and Their Reaction with Cl Atoms. *J. Phys. Chem. A* **2022**, *126*, 4585–4597.
- (19) Jorgensen, W. L.; Maxwell, D. S.; Tirado-Rives, J. Development and Testing of the OPLS All-Atom Force Field on Conformational Energetics and Properties of Organic Liquids. *J. Am. Chem. Soc.* **1996**, *118*, 11225–11236.
- (20) Kaminski, G. A.; Friesner, R. A.; Tirado-Rives, J.; Jorgensen, W. L. Evaluation and Reparametrization of the OPLS-AA Force Field for Proteins via Comparison with Accurate Quantum Chemical Calculations on Peptides. *J. Phys. Chem. B* **2001**, *105*, 6474–6487.
- (21) Jorgensen, W. L.; Tirado-Rives, J. Potential energy functions for atomic-level simulations of water and organic and biomolecular systems. *Proc. Nat. Acad. Sci.* **2005**, *102*, 6665–6670.
- (22) Dodda, L. S.; Cabeza de Vaca, I.; Tirado-Rives, J.; Jorgensen, W. L. LigParGen web server: An automatic OPLS-AA parameter generator for organic ligands. *Nucleic Acids Res.* **2017**, *45*, W331–W336.
- (23) Dodda, L. S.; Vilseck, J. Z.; Tirado-Rives, J.; Jorgensen, W. L. 1.14*CM1A-LBCC: Localized Bond-Charge Corrected CM1A Charges for Condensed-Phase Simulations. *J. Phys. Chem. B* **2017**, *121*, 3864–3870.
- (24) Garrec, J.; Monari, A.; Assfeld, X.; Mir, L. M.; Tarek, M. Lipid Peroxidation in Membranes: The Peroxyl Radical Does Not “Float”. *J. Phys. Chem. Lett.* **2014**, *5*, 1653–1658.
- (25) Plimpton, S. J. Fast Parallel Algorithms for Short-Range Molecular Dynamics. *J. Comput. Phys.* **1995**, *117*, 1–19.

(26) Assali, M.; Fittschen, C. Rate Constants and Branching Ratios for the Self-Reaction of Acetyl Peroxy ($\text{CH}_3\text{C}(\text{O})\text{O}_2\cdot$) and Its Reaction with CH_3O_2 . *Atmosphere* **2022**, *13*, 186.

(27) Shallcross, D. E.; Raventos-Duran, M. T.; Bardwell, M. W.; Bacak, A.; Solman, Z.; Percival, C. J. A semi-empirical correlation for the rate coefficients for cross- and self-reactions of peroxy radicals in the gas-phase. *Atmos. Environ.* **2005**, *39*, 763–771.

(28) Iyer, S.; Rissanen, M. P.; Valiev, R.; Barua, S.; Krechmer, J. E.; Thornton, J.; Ehn, M.; Kurtén, T. Molecular mechanism for rapid autoxidation in α -pinene ozonolysis. *Nat. Commun.* **2021**, *12*, 878.

(29) Master Chemical Mechanism (MCM), Version 3.3.1; <http://mcm.york.ac.uk/>.

(30) Jenkin, M. E.; Saunders, S. M.; Pilling, M. J. The Tropospheric Degradation of Volatile Organic Compounds: A Protocol for Mechanism Development. *Atmos. Environ.* **1997**, *31*, 81–104.

(31) Saunders, S. M.; Jenkin, M. E.; Derwent, R. G.; Pilling, M. J. Protocol for the development of the Master Chemical Mechanism, MCM v3 (Part A): Tropospheric degradation of non-aromatic volatile organic compounds. *Atmos. Chem. Phys.* **2003**, *3*, 161–180.

(32) Clary, D. C. Theoretical studies on bimolecular reaction dynamics. *Proc. Nat. Acad. Sci.* **2008**, *105*, 12649–12653.

(33) Su, Y.-T.; Lin, H.-Y.; Putikam, R.; Matsui, H.; Lin, M. C.; Lee, Y.-P. Extremely rapid self-reaction of the simplest Criegee intermediate CH_2OO and its implications in atmospheric chemistry. *Nat. Chem.* **2014**, *6*, 477–483.

(34) Buras, Z. J.; Elsamra, R. M. I.; Green, W. H. Direct Determination of the Simplest Criegee Intermediate (CH_2OO) Self Reaction Rate. *J. Phys. Chem. Lett.* **2014**, *5*, 2224–2228.

(35) Ting, W.-L.; Chang, C.-H.; Lee, Y.-F.; Matsui, H.; Lee, Y.-P.; Lin, J. J.-M. Detailed mechanism of the $\text{CH}_2\text{I} + \text{O}_2$ reaction: Yield and self-reaction of the simplest Criegee intermediate CH_2OO . *J. Chem. Phys.* **2014**, *141*, 104308.

Recommended by ACS

Electronically Nonadiabatic Effects on the Quantum Dynamics of the $\text{H}_a + \text{BeH}_b^+ \rightarrow \text{Be}^+ + \text{H}_a\text{H}_b$; $\text{H}_b + \text{BeH}_a^+$ Reactions

Ye Mao, Maodu Chen, *et al.*

AUGUST 10, 2022
THE JOURNAL OF PHYSICAL CHEMISTRY A

READ 

Rate Coefficients for $\text{OH} + \text{NO} (+\text{N}_2)$ in the Fall-off Regime and the Impact of Water Vapor

Wenyu Sun, John N. Crowley, *et al.*

JUNE 08, 2022
THE JOURNAL OF PHYSICAL CHEMISTRY A

READ 

Rovibrational-Specific QCT and Master Equation Study on $\text{N}_2(\text{X}^1\Sigma_g^+) + \text{O}(\text{P})$ and $\text{NO}(\text{X}^2\Pi) + \text{N}(\text{S})$ Systems in High-Energy Collisions

Sung Min Jo, Marco Panesi, *et al.*

MAY 23, 2022
THE JOURNAL OF PHYSICAL CHEMISTRY A

READ 

Kinetic Study of the Gas-Phase $\text{C}(\text{P}) + \text{CH}_3\text{CN}$ Reaction at Low Temperatures: Rate Constants, H-Atom Product Yields, and Astrochemical Implications

Kevin M. Hickson, Valentine Wakelam, *et al.*

APRIL 02, 2021
ACS EARTH AND SPACE CHEMISTRY

READ 

Get More Suggestions >